

# Construction and Testing of a Specific Viscosity Detector for Size Exclusion Chromatography

T. A. CHAMBERLIN and H. E. TUINSTRA, *The Dow Chemical Company, Central Research, Organic Specialties Laboratory, Midland, Michigan 48640*

## Synopsis

This article describes our experiences incorporating a viscosity detector directly within a conventional differential refractive index (DRI) detector. This results in a system in which the collection of the necessary data for universal calibration in size exclusion chromatography (SEC) can be readily attained. The system described is constructed from available materials, and yields output which can be used directly in the calculation of the intrinsic viscosity of the eluant from a chromatographic column. Values for various polymer molecular weight distribution parameters, as well as reasonable estimates of the Mark-Houwink constants, can be obtained. Additionally, a measurement related to long-chain branching in the polymer is available using this method.

## INTRODUCTION

Over the past several years, there has been renewed activity in the application of Benoit's universal calibration technique<sup>1</sup> in size exclusion chromatography. The most promising of this activity has followed the lead of Ouanno,<sup>2</sup> utilizing pressure drop across a capillary as the primary measurement of viscosity.<sup>3-19</sup> A commercial device<sup>20,21</sup> has even appeared which is claimed to be useful in this application.

There are several advantages to the application of this technique over the conventional SEC methods. These include a more accurate determination of the molecular weight distribution parameters, measurement of the whole sample intrinsic viscosity, determination of the Mark-Houwink parameters of the polymer-solvent system, and, in some instances, a measurement related to branching in the polymer. Additionally, it is possible to derive a measurement of the more inaccessible viscosity average molecular weight  $\bar{M}_v$ :

$$\bar{M}_v = \left[ \frac{\sum h_i (M_i)^a}{\sum h_i} \right]^{1/a}$$

where  $h_i$  is the peak height of a given effluent element,  $M_i$  is the corresponding molecular weight, and  $a$  is the Mark-Houwink exponent for the polymer/solvent combination being examined.

In this paper we report on the construction of a device which adequately measures these parameters, and have developed the necessary techniques and software to reduce the collected data to the desired parameters.

TABLE I  
Molecular Weight Parameters for Narrow Polystyrene Samples

Sample no.	$\bar{M}_n$	$\bar{M}_w$	$\bar{M}_z$
12C	2,400	—	2,220
61110	3,570	—	3,600
80134	9,050	—	9,100
41220	15,100	20,400	17,400
60917	51,200	53,700	47,400
70111	92,600	93,100	98,700
50124	218,000	254,000	233,000
3B	350,000	392,000	383,000
60914	600,000	599,000	607,000
61124	1,790,000	—	1,750,000

## EXPERIMENTAL

### Solutions

Samples were prepared as weight percent solutions in the appropriate solvent. Injections were carried out using Hamilton syringes (Reno, NV) and partial volume injection techniques (100  $\mu$ L loop volume). At no time was the loop filled to more than 30% of its total volume. A variety of column configurations were used. Tetrahydrofuran (THF) and chloroform ( $\text{CHCl}_3$ ) were available from Burdick and Jackson (Muskegon, MI).

### Polymers

Narrow distribution samples of polystyrene were obtained from Analabs (North Haven, CT). Reported molecular weights for these samples are shown in Table I.

A characterized broad distribution polystyrene sample (PS-1683) was obtained locally. This sample has been characterized by chromatography, ultracentrifugation, light scattering, and SEC-low-angle-laser light scattering (LALLS).<sup>22</sup> The sample is identical to one used in ASTM method D3536-76 and has been submitted to the National Bureau of Standards for certification as an NBS polymer standard. The measured molecular weight distribution parameters are listed in Table II.

Samples of branched polystyrenes were obtained from our Analytical Laboratory. These samples were prepared by polymerization in the presence of controlled amounts of divinyl benzene (DVB). The resulting polymers have

TABLE II  
Broad Standard Polystyrene

Technique	$\bar{M}_n$	$\bar{M}_w$	$\bar{M}_z$
SEC	100,000	250,000	432,000
Ultracentrifuge	100,000	250,000	—
Light scattering	—	256,000	—
SEC—LALLS	—	252,000	—

TABLE III  
Branched Polystyrene Samples

Sample	DVB (ppm)	$\bar{M}_w$ (conv.)	$\bar{M}_w$ (SEC-LALLS)	$\bar{M}_w$ (LALLS)
GP78	78	287,000	315,000	331,000
GP175	175	271,000	315,000	314,000
GP325	325	254,000	317,000	313,000

TABLE IV  
Commercial Polymer Samples

Polymer	Sample ID	$\bar{M}_n$	$\bar{M}_w$
Polycarbonate	035C <sup>a</sup>	13,400	33,800
Poly(methyl methacrylate)	037C <sup>a</sup>	84,600	60,600
Polystyrene	039C <sup>a</sup>	84,600	321,000
Poly(vinyl chloride)	038C <sup>a</sup>	37,400	83,500
Poly(vinyl acetate)	024C <sup>a</sup>	47,700	195,000
Poly(vinyl acetate)	15733 <sup>b</sup>	—	435,000
Poly(vinyl butryal)	15734 <sup>b</sup>	—	116,000
Poly(vinyl formal)	15737 <sup>b</sup>	—	47,200

<sup>a</sup>Scientific Polymer Products, Inc., Webster, NY.

<sup>b</sup>Polysciences, Inc., Warrington, PA.

been characterized by conventional (linear polystyrene calibrated) SEC, SEC-LALLS, and whole sample LALLS. These results are shown in Table III.

A number of commercially available polymer samples, listed in Table IV, were examined.

### Columns

Several column configurations were used during the course of this study. (1) Aquapore: a four-column set of Aquapore-OH columns (Brownlee Labs, Santa Clara, CA), each 4.6 mm × 25 cm, containing 10 μm particles (10, 50, 1000 and 4000 Å pore sizes). (2) PL-gel: a two-column set (7.5 mm × 30 cm, 10 μm, mixed pore distribution) of PL-gel columns (Polymer Laboratories, Ltd., Amherst, MA). (3) Ultrigel: a two-column set (4.7 mm × 30 cm, 10 μm, mixed pore distributions) of MXL and MXH Ultrigel (Analytical Sciences, Inc., Santa Clara, CA). (4) TSK-GMH6: a mixed pore distribution crosslinked polystyrene column (7.5 mm × 30 cm, 10 μm, Varian Instrument Group, Palo Alto, CA). (5) Bimodal: a two column set of silanized porous glass columns (6.2 mm × 25 cm, 8 μm, 60 and 1000 Å pores) DuPont Zorbax Bimodal II (DuPont Instruments, Wilmington, DE).

## DETECTOR CONSTRUCTION

### Detector Cell

Most workers in this area have coupled the measurement of specific viscosity to polymer concentration by using differential refractive index (DRI)

devices. In this study, a Waters model 401 differential refractometer (Milford, MA) with a detector volume of approximately 10  $\mu\text{L}$  was used. A stainless capillary with dimensions  $24 \times 0.006$  in. ID (approximately 10  $\mu\text{L}$ ) connected to two zero-volume, three-way fittings along with the appropriate connectors for attachment to a differential pressure transducer and to the rest of the chromatographic system, was obtained from Supelco (Supelco, Inc., Bellefonte, PA. P/N 5-8269, sample valve capillary bypass). We have successfully used such systems either attached directly downstream from the SEC columns or incorporated within the DRI detector itself.

### Dual Detector

The concurrent measurement of specific viscosity and polymer concentration in the eluent from an SEC column can be confounded by at least three factors. One of these is the temperature variation during the viscosity measurement. Based on viscosity-temperature coefficients for tetrahydrofuran<sup>23</sup> and an exponential relationship between temperature and viscosity, a specific viscosity change of 0.0002 would be associated with a temperature change of 0.02°C. Another factor is incorrect accommodation of the volumetric offset between the two detectors,<sup>10</sup> and a third is sample dilution during transport between the two detectors.<sup>24</sup> To minimize these three factors, we incorporated the capillary directly into the Waters 401 DRI detector.

The detector was dismantled, and the solder melted from the channel leading the two inlet lines to the bottom of the detector stage. Next, space was milled in the aluminum block for the capillary, zero volume tees, and associated plumbing (see Fig. 1). The capillary system was installed, recast in solder, and the electronic and optical components of the detector were re-assembled. The line from the low-pressure end of the capillary to the bottom of the DRI detector stage consisted of 15 cm of 0.01 in. ID tubing (7.6  $\mu\text{L}$ ). This arrangement affords good temperature stability (most of the mass of the DRI detector is used as thermal ballast) and minimizes both the volumetric offset between the detectors and the sample back mixing during transport between detectors.

It is important to keep the volume of the two detectors small and as identical as possible so that no corrections need be considered during workup of the collected data. Other workers have used viscosity detector volumes of 25<sup>3</sup>, 120<sup>5</sup>, 15<sup>13</sup>, and 62<sup>19</sup>  $\mu\text{L}$ . Under typical conditions for most of our analyses (i.e., THF at 1.0 mL/min.), flow through the viscosity detector was laminar (Reynolds number  $\approx 45$ ).

### Differential Transducer

The high and low pressure lines from the dual detector were connected to the appropriate ports of a Validyne DP-15 variable reluctance differential pressure transducer (Validyne Eng. Corp., Northridge, CA). The transducer was operated in the wet/wet mode by carefully filling the lines and cavities with solvent. The transducer was activated and a corresponding signal generated using a Validyne CD-101 carrier demodulator. The signal from this system was divided to some desired value (usually 200–1000 mV) and then bucked to zero, using suitably divided output from a constant voltage source.

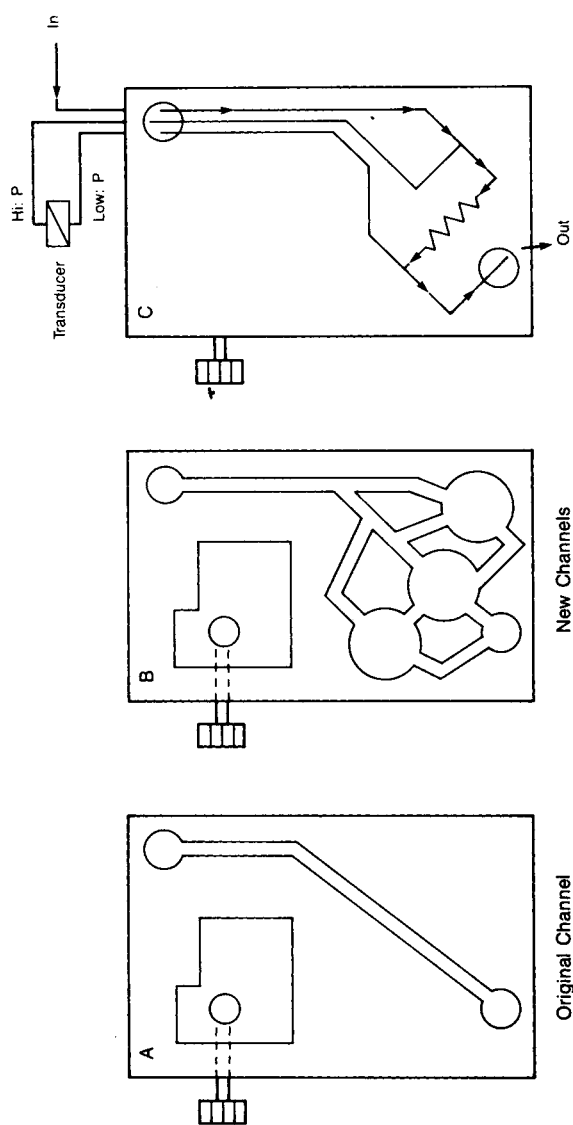


Fig. 1. Schematic of modifications made to Water's model 401 differential refractive index detector: (A) bottom view of thermal ballast portion of detector; (B) layout of milled portion detector block; (C) flow schematic of installed viscosity detector.

In this way, it was possible to arrange the system so that a flow of 1.0 mL/min (nominal) is associated with a 500 mV output from the transducer, while the recorder (or microprocessor) monitored changes in signal level of 10 mV (2% full scale).

For systems maintaining constant flow, changes in the differential pressure are directly related to changes in viscosity of the medium generating the differential pressure.<sup>2</sup> For a typical case (e.g., baseline = 500 mV), a polymer solution with a specific viscosity of 0.004 would generate a 2 mV reading on the data collection system.

The remainder of the system was constructed of typical equipment used for SEC. An LCD Constametric III pump (Milton Roy Co., Riviera Beach, FL) was damped with an LDC Mark III and a Lichroma-Damp II to suppress the flow noise caused by the pump. A Rheodyne 7125 injection valve (Rheodyne Inc., Cotati, CA) was connected to the SEC columns which were connected in turn to the dual detector. Output from the dual detector (both DRI and differential pressure) was collected using both a recorder and a Digital Equipment Corp. DEC LSI/1123 laboratory computer (Marlboro, MA). Columns and as much of the connecting tubing as possible were thermostatted at  $25.0 \pm 0.01^\circ\text{C}$  using a water bath. Elution volumes were measured using a thermal pulse time-of-flight technique.<sup>25,26</sup>

## TESTING OF THE SYSTEM

### System Noise

Figures 2 and 3 depict short and long-term noise inherent in the viscosity detector described to this point. The more critical short-term noise (Fig. 2) amounts to about 0.02%–0.04% of the total output from the transducer at a flow rate of 1.0 mL/min. This represents a variance in specific viscosity of 0.0002–0.0004, the same magnitude as expected from temperature fluctuations in the system.

The observed long-term noise (Fig. 3) is a little larger than the short-term noise, containing occasional excursions on the order of 0.1%. We feel that these

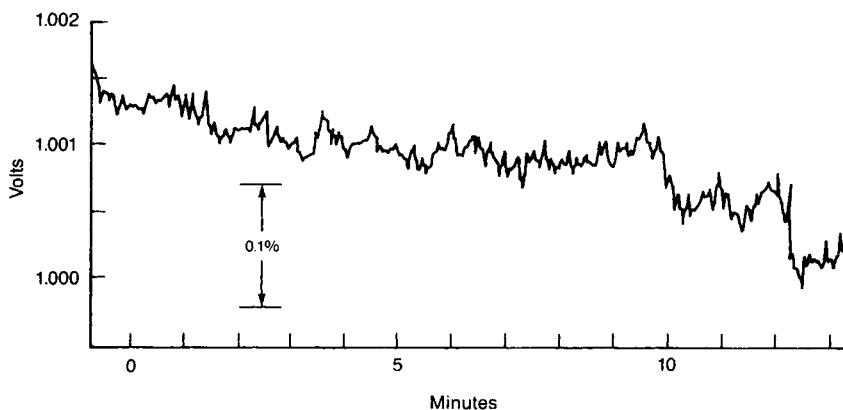


Fig. 2. Short term flow noise associated with the viscosity detector. Nominal flow rate of 1.0 mL/min.

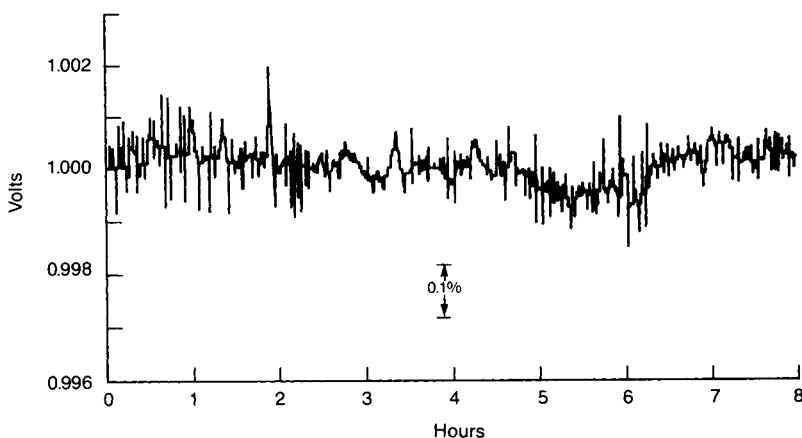


Fig. 3. Long term flow noise associated with the viscosity detector. Nominal flow rate of 1.0 mL/min.

variations are due to check valves failing to seat properly on a somewhat random basis.

### Flow-Rate Detection

It is obvious that in the absence of any changes in viscosity, the described detector can be considered a flow detector. We chose to use this property as a method to test the response of the detector. Since pressure drop across a capillary is linear in both viscosity and flow rate, we concluded that linear

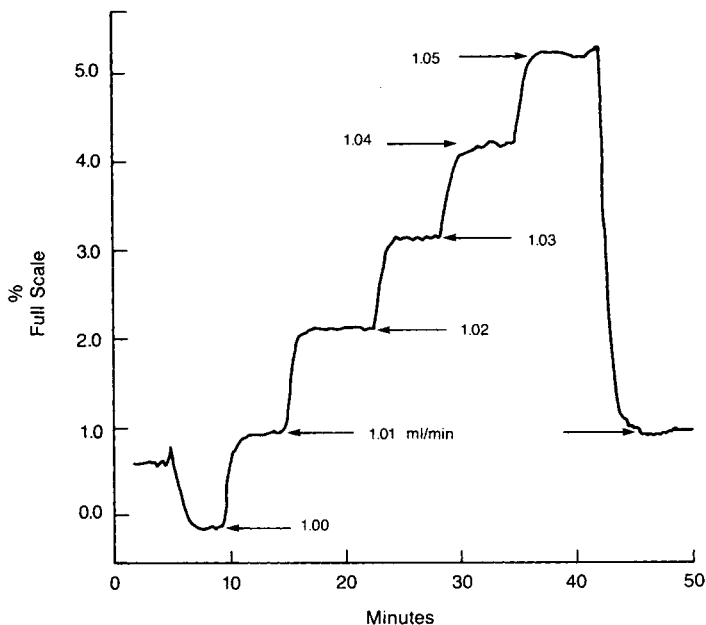


Fig. 4. Signal from viscosity detector utilized in the flow rate detection mode. Tetrahydrofuran at 25.0°C; arrows indicate pump settings used to generate flow rates.

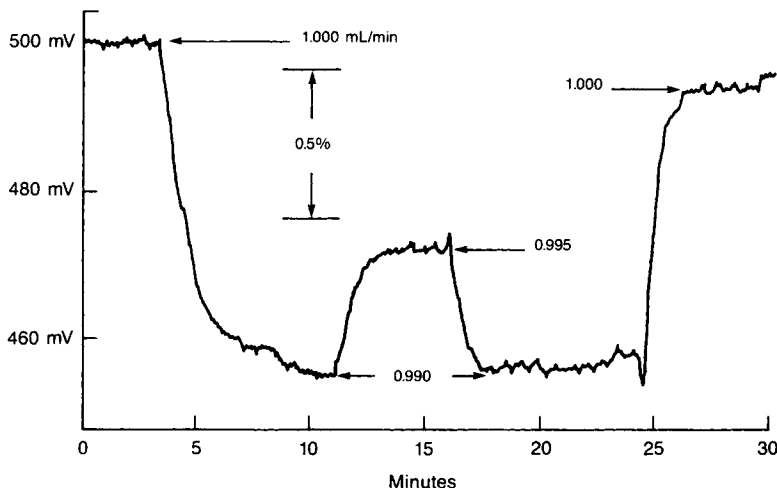


Fig. 5. Smaller flow rate changes as measured using the viscosity detector. Same conditions as shown in Figure 4.

response to flow rate changes (at constant solution viscosity) would be equivalent to linear response to viscosity changes at constant flow rate.

Figure 4 depicts the results of changing the pump setting incrementally from 1.00 to 1.05 mL/min. At the beginning of the experiment, the detector output was adjusted so that a change in pressure drop of 10% would result in full scale deflection on the recorder (i.e., 10 mV). From this result, we concluded that indeed the detector did respond as anticipated. Figure 5 shows our results when an even finer perturbation was made to the system (full scale

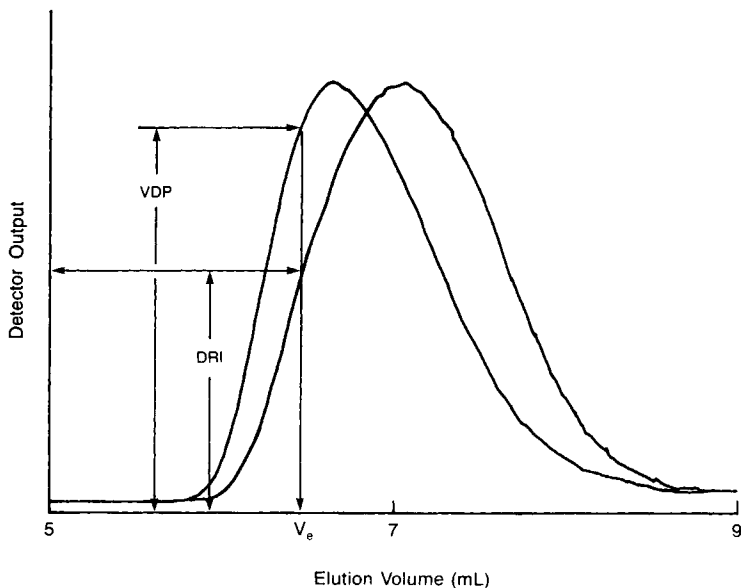


Fig. 6. Dual detector output for 200  $\mu$ g injection of a broad PS-1683 polystyrene sample. Nominal flow rate of 1.0 mL/min, tetrahydrofuran, 25.0°C, Dupont Bimodal-S column set.



deflection for this experiment was adjusted to 2%). In this case, the response was not as accurate as we had hoped, although this lack could also be due to mechanical problems in the mechanism for adjusting the pump setting.

### Dual Detection

Figure 6 shows the output from the dual detector generated from a 200  $\mu\text{g}$  sample of PS-1683. The specific viscosity of the effluent element is derived from the viscosity differential pressure (VDP) measurement. The amount of polymer generating the VDP output is determined based on the amount of polymer injected and the normalized signal of the differential refractive index (DRI) detector. Because of the dilute nature of the effluent, it is sufficient to relate the intrinsic viscosity to the ratio of the two detector signals:

$$[\eta] = k(\text{VDP}_i/\text{DRI}_i)$$

where  $k$  contains the appropriate geometric, injection, and concentration constants relative to this particular sample, and the subscript indicates the solution element being examined.

If the column arrangement has been previously calibrated, then the elution volume ( $V_e$ ) can be related to a hydrodynamic size as was shown by Grubisic et al.<sup>1</sup> This size is defined as the product of molecular weight and intrinsic viscosity. Having a measurement of "size" (via elution volume measurement and calibration equation) as well as a measure of intrinsic viscosity (from the dual detector system), we can directly measure molecular weight.

Figure 7 contains a plot of the observed specific viscosity of the effluent versus the amount (concentration) of polymer eluting from the system for an injected sample of 100  $\mu\text{g}$  of 100,000  $\bar{M}_w$  low dispersity polystyrene. If dispersion in the column is minimal and if the sample is truly narrow, this

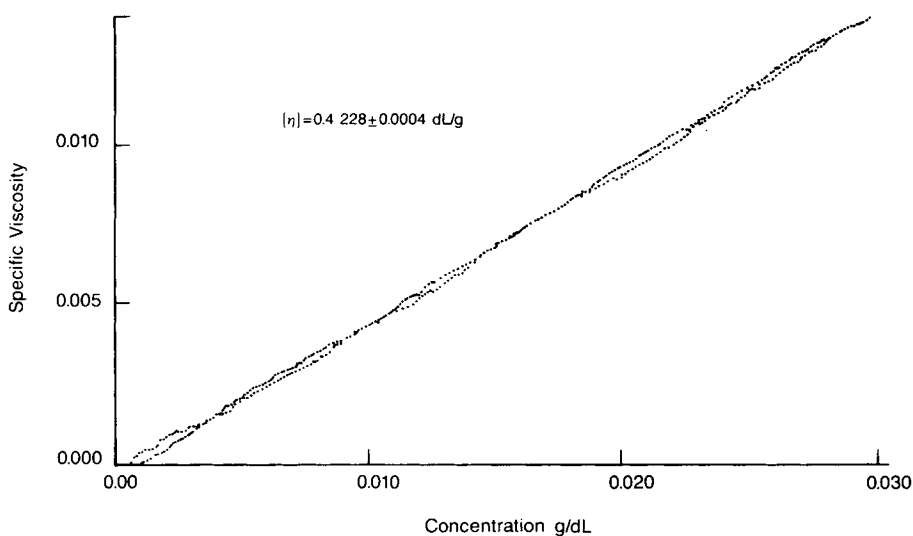


Fig. 7. Mark-Houwink plot generated from narrow molecular weight distribution sample of 100,000  $\bar{M}_w$  polystyrene. Tetrahydrofuran (25°C), 1.00 mL/min.

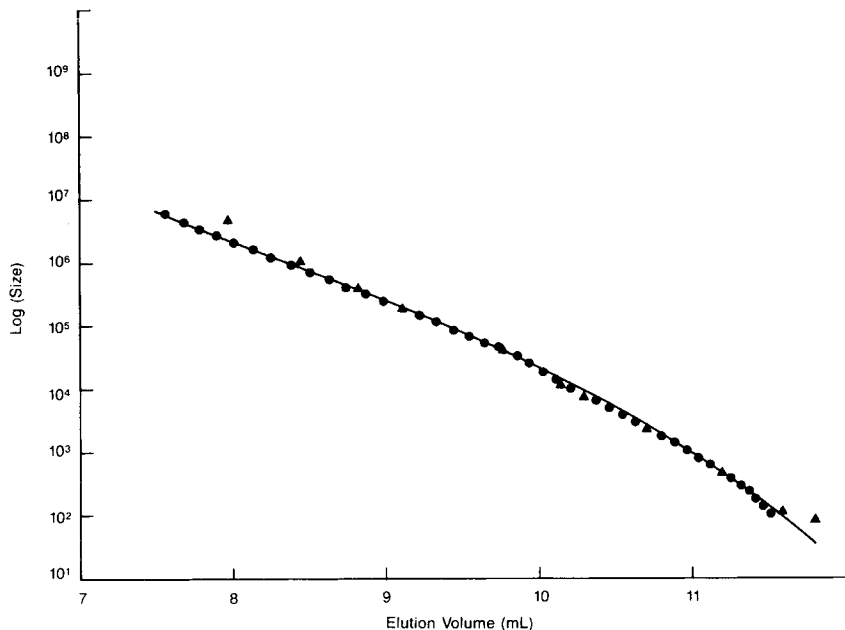


Fig. 8. Calibration results using third order in elution volume and third order in injected mass calibration equation: (●) derived from broad sample; (▲) derived from narrow standards samples; (—) generated from calibration equation.

plot should be linear with a slope equal to the intrinsic viscosity of the sample-solvent combination. The observed linear plot ( $r = 0.9996$ ), has a slope of  $0.423 \text{ dL/g}$ . Polystyrene of  $100,000 \bar{M}_w$  in THF at  $25.0^\circ\text{C}$  has Mark-Houwink constants  $k = 15.3 \times 10^{-5} \text{ dL/g}$  and  $\alpha = 0.681$ .<sup>22</sup> This yields a calculated intrinsic viscosity of  $0.389 \text{ dL/g}$ . Other values for the Mark-Houwink constants<sup>27</sup> ( $16.0$  and  $14.1 \times 10^{-5} \text{ dL/g}$  for  $k$  and  $0.700$  for  $\alpha$ ) yield calculated intrinsic viscosities of  $0.506$  and  $0.446$ . This close correspondence between calculated and observed values for intrinsic viscosity support to this particular approach.

### Calibration

For all the various column configurations studied, a broad standard calibration technique was used.<sup>28</sup> In general, four to six injections of varying amounts of polymer were made and the collected data subjected to regression analysis using a model containing first through third order terms in both amount of polymer and elution volume. The calibration equation used is

$$\ln(M_w[\eta]) = f(V, V^2, V^3) \cdot g(\mu g, \mu g^2, \mu g^3)$$

For a column configuration consisting of a Waters E-high followed by a DuPont Bimodal-S pair, this calibration approach led to the results shown in Figure 8. In this figure, the circles represent the 43 characterized portions of the PS-1683 polystyrene sample for an injection of  $180 \mu\text{g}$  of polymer. The triangles represent the elution volume-hydrodynamic volume relationship of

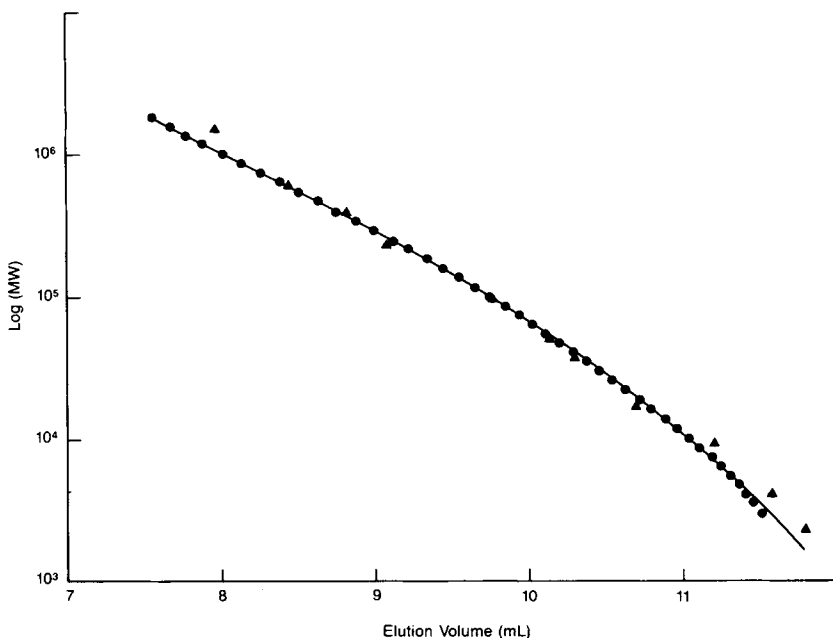


Fig. 9. Conventional calibration plot using both broad and narrow standard samples. All injections contained  $180 \mu\text{g}$  polymer.

$180 \mu\text{g}$  injections of the narrow standard polystyrene samples shown in Table I. Known molecular weights were converted to hydrodynamic volume by combination with the observed intrinsic viscosities. The solid line in Figure 8 is the line generated using  $180 \mu\text{g}$  and the calculated coefficients from the regression analysis mentioned above.

Figure 9 contains a "conventional" calibration plot using a third order in elution volume relationship between molecular weight and elution volume. In this case, sample loading effects have been ignored.

### Analysis

It is an inherent property of the dual detector that the extremes of a sample are less well defined. This occurs because, at the high molecular weight end of any distribution, the viscosity detector is more sensitive than the concentration detector. The opposite is true at the low molecular weight end of the sample. Because of this, we have found that, for determination of the Mark-Houwink coefficients for a system, it is beneficial to use only the central 90% of the DRI signal generated by the eluting sample. This can best be explained by referring to Figure 10.

Figure 10 is a plot of the observed intrinsic viscosity against the molecular weight derived from the calibration plot, the elution volume, and the observed intrinsic viscosity as previously discussed. The two marks located along the curve enclose the middle 90% of the observed DRI output. The scatter of the data around the derived line at the low  $M_w$  end of the plot is due to the signal-to-noise ratio of the viscosity detector under these conditions.

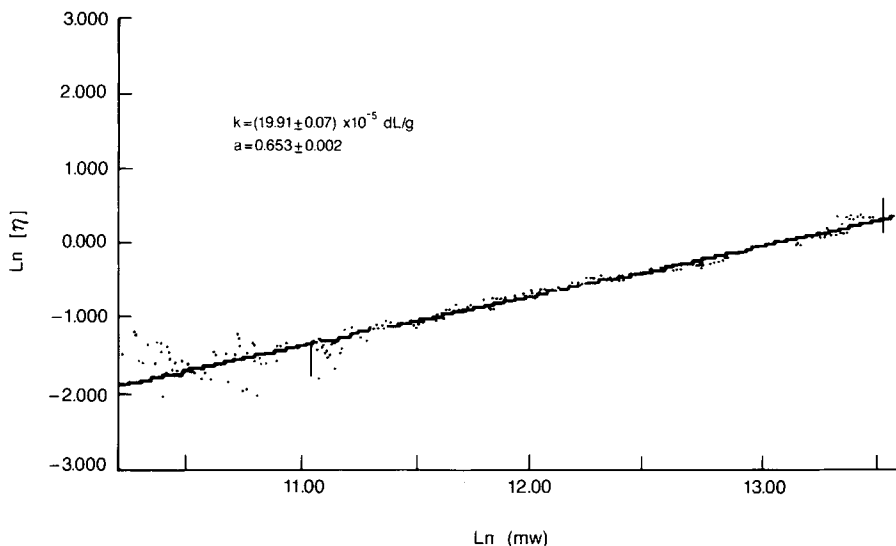


Fig. 10. Mark-Houwink plot for data shown in Figure 6. Parameters estimated using data from broad standard sample and narrow standard samples (see Fig. 8).

The coefficients derived from the data are acceptable ( $k = 19.9 \times 10^{-5}$  dL/g,  $a = 0.653$ ). Using these coefficients and the output from the mass detector, we can calculate several molecular weight distribution parameters (see Fig. 11). In this figure are reported the various calculated values derived from this approach. Also shown are the two baseline points chosen, as well as the peak maximum (max). The remaining two marks along the DRI trace enclose the region of data used to calculate the Mark-Houwink coefficients.

Several different amounts of PS-1683 were analyzed in this manner, varying in both concentration and injection size. The results, as shown in Table V, demonstrate that this technique gives values for the various molecular weight

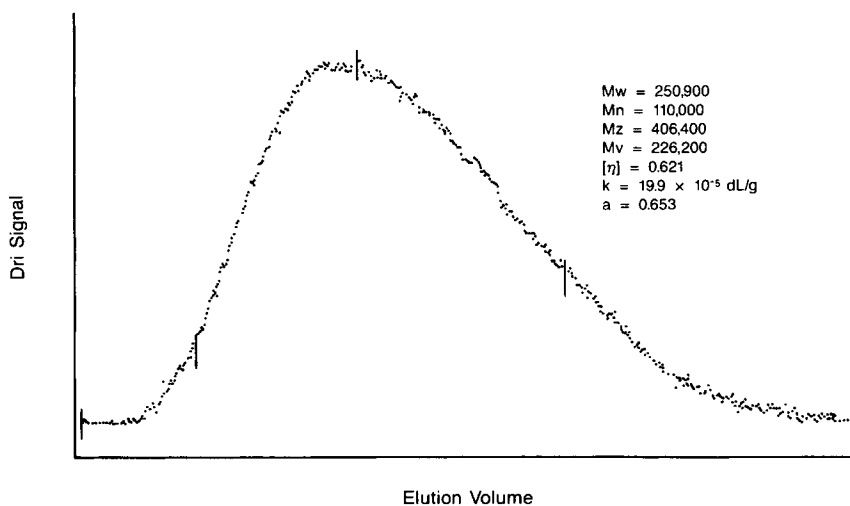


Fig. 11. Typical output from an analysis. Same sample as used to generate Figs. 8 and 9.

TABLE V  
 Analysis of Broad Polystyrene Samples ( $\bar{M} \times 10^{-3}$ )

Run	$\bar{M}_n$	$\bar{M}_w$	$\bar{M}_z$	$\bar{M}_v$	$[\eta]$	$k \times 10^{-5}$	$\alpha$
1	95.4	265	453	222	0.679	39.0	0.606
2	99.7	249	434	219	0.690	30.6	0.628
3	102	248	426	221	0.696	24.8	0.645
4	103	251	428	226	0.670	13.9	0.688
Ave.	100	251	435	222	0.684	27.1	0.642
St. dev.	3.3	3.6	12.2	3.0	0.012	10.5	0.035
True	100	250	432	209	0.663	15.3 <sup>26</sup>	0.681 <sup>26</sup>

distribution parameters which are in complete accord with accepted values. The reproducibility of most of these parameters is generally less than 5%. The greatest variation is observed in the Mark-Houwink coefficients, and is probably due to the long extrapolation along a logarithmic axis.

Results from several characterized polymers are shown in Table VI. Quite surprisingly, we found that several of the "characterized" commercially available polymers were incorrectly labeled. The column headed  $\bar{M}_w$  (LALLS) contains the molecular weight of the various polymers determined using a whole sample LALLS technique.<sup>29</sup> In three of the samples [poly(vinyl formal), poly(methyl methacrylate), and poly(vinyl butyral)], grossly incorrect molecular weight values were supplied.

In general, the correspondence between  $\bar{M}_w$  (LALLS) and  $\bar{M}_w$  (SEC- $[\eta]$ ) shown in Table VI was good, although not as accurate as we had wished. It is possible that some of the variance was due to column resolution. In order to examine this possibility, a series of column configurations were examined. The data, shown in Table VII, seems to indicate that the accuracy of the results is a function of the resolution of the column configurations used. No accommodation for band spreading has been incorporated in the software, perhaps leading to some of the above inaccuracies. In general, however, it appears that the SEC- $[\eta]$  approach does yield reasonably accurate results.

The concepts behind the universal approach to polymer SEC indicate the technique should be solvent independent. To demonstrate this,  $\text{CHCl}_3$  was

 TABLE VI  
 $\bar{M}_w$  Values of Commercial Polymers<sup>a</sup>

Polymer	$\bar{M}_w$ (supplier)	$M_w$ (LALLS)	$\bar{M}_w$ (SEC- $[\eta]$ )
Polycarbonate	33.8	20.5	29.5
Poly(vinyl formal)	47.2	70.9	77.5
Poly(vinyl chloride)	83.5	78.0	99.5
Polystyrene	321	337	295
Poly(methyl methacrylate)	60.6	94.7	110
Poly(vinyl acetate)	195	202	221
Poly(vinyl butyral)	116	55.8	70.8

<sup>a</sup> TSK GMH6, THF, 1.0 mL/min,  $\bar{M}_w \times 10^{-3}$ .

TABLE VII  
 $\bar{M}_w$  Values Obtained Using Various Column Configurations<sup>a</sup>

Polymer	LALLS	TSK-GMH6	PL-gel	Aquapore	Bimodal	Ultrage
Polycarbonate	20.5	29.5	19.2	32.1	32.3	23.2
Poly(vinyl formal)	70.9	77.5	62.9	66.9	73.0	68.1
Poly(vinyl chloride)	78.0	99.5	89.4	94.8	81.9	82.2
Polystyrene	337	295	336	301	326	254
Poly(methyl methacrylate)	94.7	110	107	123	123	91.9
Poly(vinyl acetate)	202	221	223	217	234	190
Poly(vinyl butryal) <sup>a</sup>	55.8	70.8	88.0	69.8	75.4	56.0

(THF, 1.0 mL/min,  $\bar{M}_w \times 10^{-3}$ ).

<sup>a</sup>(THF, 1.0 mL/min,  $\bar{M}_w \times 10^{-3}$ ).

 TABLE VIII  
 Effect of Solvent on  $\bar{M}_w$  Measurement<sup>a</sup>

Polymer	LALLS	THF	CHCl <sub>3</sub>
Polycarbonate	20.5	19.2	39.4
Poly(vinyl butryal)	55.8	88.0	59.0
Poly(methyl methacrylate)	94.7	107	112
Polystyrene	337	336	337
Poly(vinyl acetate)	202	223	205

<sup>a</sup>PL-gel, 1.0 mL/min,  $\bar{M}_w \times 10^{-3}$ .

used as SEC mobile phase. The results are shown in Table VIII. As expected, there was fairly good agreement between the THF and CHCl<sub>3</sub> mobile phases, except for polycarbonate.

Table IX contains the results obtained from branched polystyrenes using the dual detector system. As expected, the measured intrinsic viscosity for the branched samples  $[\eta]_b$  decreased with increasing incorporation of the cross-linker, divinyl benzene.<sup>30</sup>

Using the method of Ambler et al.<sup>31</sup>, it is possible to estimate parameters related to the branching in the above samples. These workers used relationships derived by Zimm and Stockmayer,<sup>32</sup> which led to the following functions:

$$[\eta]_{\text{branched}}/[\eta]_{\text{linear}} = g^{1/2}$$

$$g = \left[ (1 + m/7)^{1/2} + 4m/9\pi \right]^{-1/2}$$

 TABLE IX  
 Analysis of Branched Polystyrene Samples<sup>a</sup>

DVB (ppm)	LALLS	$\bar{M}_n$	$\bar{M}_w$	$\bar{M}_z$	$\bar{M}_v$	$[\eta]$	$k \times 10^{-5}$	$a$
0	330	123	289	479	257	0.761	33.3	0.621
78	331	138	315	569	274	0.734	38.3	0.604
175	314	108	296	613	247	0.685	71.8	0.553
325	313	91.1	303	707	241	0.597	61.6	0.555

<sup>a</sup>Bimodal, THF, 1.0 mL/min,  $\bar{M}_w \times 10^{-3}$ .

TABLE X  
Branching Functions for Lightly Crosslinked Polystyrene Samples

DVB (ppm)	$[\eta]$	$[\eta]_b/[\eta]_l$	$g$	$m$	$\lambda^a$	$\lambda^b$
0	0.761	1.000	1.000	0.00	0.00	0.00
78	0.734	0.965	0.930	0.74	0.26	0.36
175	0.685	0.900	0.810	2.52	0.87	0.81
325	0.597	0.785	0.615	8.23	2.85	1.50

<sup>a</sup> Calculated for a molecular weight of 300,000.

<sup>b</sup> Assumes each DVB monomer contributed two branches to the chain.

where  $m$  is the number of branch points in a given molecule with intrinsic viscosity  $[\eta]_{\text{branched}}$ ,  $[\eta]_{\text{linear}}$  is the intrinsic viscosity of the corresponding linear polymer with the same molecular weight  $M$ . The branching frequency  $\lambda$ , for a given molecular weight is defined as

$$\lambda = m/M$$

The ratio of branched and linear intrinsic viscosities can be taken from Table IX. Assuming that 300,000- $M_w$  polymer was prepared in all instances, and solving, using the observed value for  $g$ , leads to the branching frequencies shown in Table X.

Although the calculated branching frequency for the most highly branched sample is substantially different from that which is obtained from this technique, we feel that the technique does yield information concerning the number of long chain branches.

## CONCLUSION

It is reasonably simple to construct a viscosity detector for SEC. The approach described here involves the measurement of a pressure drop across a capillary and—when coupled with a DRI measurement of polymer mass—can be converted directly into intrinsic viscosity. Most of the problems associated with the measurement of small changes in viscosity can be overcome by placing the capillary directly inside the thermal ballast of the DRI detector.

The authors would like to acknowledge S. Martin and E. North from our Analytical Laboratory for carrying out the LALLS and SEC-LALLS experiments reported above. Additionally, we would like to thank them for supplying branched polystyrene samples.

## References

1. Z. Grubisic, P. Rempp, and H. Benoit, *J. Polym. Sci.*, **5**, 753 (1967).
2. A. C. Ouanno, *J. Polym. Sci., Polym. Symp.*, **43**, 299 (1973).
3. A. C. Ouanno, D. L. Horne, and A. R. Gregges, *J. Polym. Sci. Polym. Chem. Ed.*, **12**, 307 (1974).
4. J. Leseq and C. Quivoron, *Analysis*, **4**, 456 (1976).
5. L. Letot, J. Leseq, and C. Quivoron, *J. Liq. Chromatogr.*, **3**, 427 (1980).
6. L. Letot, J. Leseq, and C. Quivoron, *J. Liq. Chromatogr.*, **3**, 1637 (1980).
7. D. Lecacheux, J. Leseq, and C. Quivoron, *Am. Chem. Soc. Polym. Prepr.*, **23**, (2), 126 (1982).
8. D. Lecacheux, J. Leseq, and C. Quivoron, *J. Appl. Polym. Sci.*, **27**, 4867 (1982).
9. D. Lecacheux, J. Leseq, and C. Quivoron, *J. Liq. Chromatogr.*, **5**, 217 (1982).

10. D. Lecacheux and J. Leseq, *J. Liq. Chromatogr.*, **5**, 2227 (1982).
11. D. Lecacheux, J. Leseq, and C. Quivoron, *J. Appl. Polym. Sci.*, **29**, 1569 (1984).
12. F. B. Malihi, M. E. Koehler, C. Kuo, and T. Provder, 1982 Pittsburgh Conf., paper 806.
13. F. B. Malihi, C. Kuo, M. E. Koehler, T. Provder, and A. F. Kah, *Org. Coat. Div. Am. Chem. Soc. Mtg.*, **48**, 760 (1983).
14. M. E. Koehler, A. F. Kah, T. F. Niemann, C. Kuo, and T. Provder, *Org. Coat. Div. Am. Chem. Soc. Mtg.*, **48**, 617 (1983).
15. C. Kuo, F. B. Malihi, T. Provder, M. E. Koehler, and A. F. Kah, *FACSS 10th Mtg.*, Sep. 1983, paper 231.
16. F. B. Malihi, C. Kuo, M. E. Koehler, T. Provder, and A. F. Kah, *Org. Coat. Appl. Polym. Sci. Proc.*, **48**, 760 (1983).
17. F. B. Malihi, C. Kuo, M. E. Koehler, T. Provder, and A. F. Kah, *Am. Chem. Soc. Symp. Ser.*, **245**, 281 (1984).
18. H. W. Johnson, Jr., (Shell Oil Co.), U.S. Pat. 4,286,457 (1981).
19. G. Callec, A. W. Anderson, and G. T. Tsao, *J. Polym. Sci. Polym. Chem. Ed.*, **22**, 287 (1984).
20. M. A. Haney, *Am. Chem. Soc. Polym. Prepr.*, **24** (2), 455 (1983).
21. M. A. Haney, *J. Appl. Polym. Sci.*, **30**, 3037 (1985).
22. E. North, Dow Chemical Co., Midland, MI, private communication.
23. Beilstein, **17**(iii/iv), 26 (1974).
24. R. Bressau, *Chromatogr. Sci. Ser.*, **13**, 73 (1979).
25. T. E. Miller, Jr., and H. Small, *Anal. Chem.*, **54**, 907 (1982).
26. T. A. Chamberlin and H. E. Tuinstra, *Anal. Chem.*, **55**, 428 (1983).
27. W. W. Yau, J. J. Kirkland, and D. D. Bly, *Modern Size Exclusion Chromatography*, Wiley, New York, 1979, p. 336.
28. W. W. Yau, J. J. Kirkland, and D. D. Bly, *Modern Size Exclusion Chromatography*, Wiley, New York, 1979, p. 294.
29. S. Martin, Dow Chemical Co., Midland, MI, private communication.
30. W. S. Park and W. W. Graessley, *J. Polym. Sci., Polym. Phys. Ed.*, **15**, 85 (1977).
31. M. R. Ambler, R. D. Mate, and J. R. Purdon, Jr., *J. Polym. Sci., Polym. Chem. Ed.*, **12**, 1759 (1974).
32. B. H. Zimm and W. H. Stockmayer, *J. Chem. Phys.*, **17**, 1301 (1949).

Received February 18, 1987

Accepted August 17, 1987